DEEP LEVEL TRANSIENT SPECTROSCOPY

CHIN-CHE TIN

Department of Physics, Auburn University, Auburn, AL, USA

INTRODUCTION

Defects are responsible for many different characteristic properties of a semiconductor. They play a critical role in determining the viability of a given material for device applications. The identification and control of defects have always been among the most important and crucial tasks in materials and electronic device development. The performance and reliability of devices can be significantly affected by only minute concentrations of undesirable defects. Since the ultimate quality of a material depends on the sensitivity of a characterization technique, the challenge in materials characterization has been to develop detection methods with improved sensitivity.

Whereas electrical characterization methods are more sensitive than physical characterization techniques, they may arguably be less sensitive than some optical techniques. However, since device operation depends largely on the electrical properties, electrical characterization is therefore more relevant. Also, the activation of defects due to electrical processes requires scrutiny as it has a direct impact on the performance and reliability of a device.

The deep level transient spectroscopy (DLTS) technique probes the temperature dependence of the charge carriers escaping from trapping centers formed by point defects in the material. This technique is able to characterize each type of trapping center by providing the activation energy of the defect level relative to one of the energy band edges and the capture cross-section of the traps. This technique can also be used to compute the concentration and depth profiling of the trapping centers.

Although there exist several electrical characterization techniques such as Hall effect, current–voltage, capacitance–voltage, and carrier lifetime measurements, (see for example Hall Effect in Semiconductors and Capacitance-Voltage (C-V) Characterization of Semiconductors) none of them is of a spectroscopic nature. The spectroscopic nature of DLTS is a key feature that provides both convenience and sensitivity.

Deep level transient spectroscopy has been widely used for many different semiconductors. This technique has distinguished itself in contributing to the resolution of many defect-related problems in several technologically important semiconductors such as silicon, the III–V and II–VI compounds, and alloys. Many different variations of the basic DLTS technique have also been developed for improved sensitivity and for more specialized applications in device structures different from the normal p–n or Schottky barrier diodes.

DLTS is not able to identify the chemistry and the origin of a defect. DLTS data should therefore be used in conjunction with other techniques. A successful study of defects requires a concerted effort of various researchers using various characterization techniques in order to derive a more accurate and consistent picture of the defect structure of a given material.

Defects in Semiconductors

In a real crystal, the periodic symmetry of the lattice can be broken by defects. Lattice defects produce localized energy states that may have energy levels occurring within the band gap. A carrier (electron or hole) bound to such a defect in a lattice has a decaying wavefunction as opposed to a carrier in the allowed energy bands (conduction or valence bands) that is free to move.

Crystal imperfections known as point defects can be vacancies or impurities that are introduced either deliberately or unintentionally during the growth process. Processing of materials during device fabrication can also introduce point defects. Some defects are unavoidable and they play a key role in determining the properties of a semiconductor. Chemical impurities that form point defects may exist interstitially or substitutionally in the lattice. An interstitial atom may be of the same species as the atoms in the lattice (intrinsic defects) or of a different species (extrinsic defects). Defects can also be formed by vacant lattice sites. There are also defect complexes that are conglomerations of different point defects.

Besides point defects, there are also one-dimensional defects such as dislocations, two-dimensional defects such as surfaces and grain boundaries, and three-dimensional defects such as micropipes and cavities.

Defects occur in accordance with the laws of thermodynamics and the laws of mass action. Hence, the removal or suppression of one type of defect will enhance the effects of another type. For instance, the removal of defects such as grain boundaries and dislocations increases the significance of point defects.

The presence of defects in semiconductors can be either beneficial or detrimental, depending on the nature of the defects and the actual application of the material in devices.

Gold impurities in silicon junctions are used to provide fast recombination resulting in faster switching time. Impurities such as gold, zinc, mercury, etc., in silicon and germanium produce high quantum efficiency photodetectors. The emission wavelength of light-emitting diodes (LEDs) is determined by the presence of deep levels. In undoped semi-insulating GaAs, a family of deep donor levels, commonly known as EL2, compensates the acceptor level due to carbon impurity to give rise to the high-resistivity or semi-insulating property. Chromium is also used to dope GaAs to produce semi-insulating GaAs:Cr, although this is no longer in widespread use.

On the other hand, device performance and reliability are greatly affected by the presence of defects. The success of fiber optics–based telecommunication systems employing laser diodes depends critically on the lifetime of the laser diodes and LEDs. The degradation of laser diodes and LEDs has been widely attributed to formation of local regions where nonradiative recombination

Characterization of Materials, edited by Elton N. Kaufmann.

occurs. There is general agreement that these regions are due to the motion of dislocations that interact with defect centers to promote nonradiative recombinations. A dislocation array can also propagate from a substrate into the active layers resulting in device failure. This is a reason why electronic materials of low dislocation density are crucial.

Device fabrication processes usually involve ion implantation, annealing, contact formation, mechanical scribing, and cleaving, all of which introduce dislocations and point defects in one way or another. Dislocations in devices may be of little significance by themselves. The problems only arise when these dislocations are "decorated" by point defects. Impurities tend to gather around dislocations and diffusion of impurities is also enhanced at dislocations. It is difficult to differentiate between the effects of point defects and dislocations, owing to the fact that production of dislocations also generates point defects such as interstitial atoms and vacancies.

The topic of reliability and degradation of devices is wide ranging and the above examples serve only to show the significance of the studies of defect in devices.

The localized states within the band gap can range from a few millielectron volts to a few tenths of an electron volt from either the conduction or valence bands. The determination of whether a level can be considered deep or shallow is rather arbitrary. A depth of ≥ 0.1 eV is usually termed *deep level*. It must also be noted that the accuracy in the determination of any level <0.1 eV is always questionable in any experiment that involves the electrical or photoelectronic measurement of the thermal emission of carriers from the trapping levels.

A defect center can be either a recombination or a trapping center depending on the probabilities in which each of the two processes will occur. If a carrier bound to a defect center recombines with another carrier of opposite polarity before it can be thermally released to the nearest allowed energy band, then that center is a recombination center. However, if the carrier can escape to the nearest band through thermal excitation before recombination can occur, then that center is a trapping center. The probability of escape of a carrier from a defect center is therefore higher if the energy level of the center is nearer to either the valence or conduction bands. This means that a donor or acceptor level near either the valence or conduction bands is more likely to be a trapping center.

PRINCIPLES OF DLTS

DLTS was first introduced by Lang (1974, 1979) based on the theoretical groundwork of Sah et al. (1970) and Milnes (1973). The basis of this method is the dependence of the capacitance of a space charge region on the occupancy of the traps within the space charge region in a semiconductor. Under a nonequilibrium condition such as that existing in a space charge region, a trapped carrier can escape from a trapping center by thermal excitation to the nearest energy band.

To characterize a semiconductor, it is necessary to fabricate a junction diode such as a p–n or a Schottky barrier diode on the material. A space charge region is formed by reverse biasing a p–n diode or a Schottky barrier diode. The diode is initially reverse biased to empty the traps. When the bias across the junction is reduced (or even forward biased), the width of the space charge region is reduced. An equilibrium condition is established in the neutralized region with the majority carriers populating the traps. When the reverse bias is restored, the space charge region is again created as before, with the only difference that there are trapped carriers now residing in the defect centers within the space charge region. The nonequilibrium condition thus created causes the trapped carriers to be thermally reemitted to the relevant energy band. The rate of thermal emission or detrapping of a carrier is temperature dependent. The change of the occupancy of these trapping centers is reflected in the capacitance of the junction producing a capacitance transient. Minority carrier injection can also occur when the junction is forward biased during the bias pulse. In essence, both majority and minority carriers are involved that makes this method all the more effective because the emission of each type of carrier can be detected by monitoring the capacitance transients. The activation energy of the trap, or the depth of the trapping level from the nearest energy band edge, and the capture cross-section can be determined from the temperature dependence of the emission rate. The trap concentration can be determined from the intensity of the capacitance peak and the polarity of the carriers can be found from the sign of the capacitance change. The DLTS technique can be applied to the study of trapping centers along a critical current conduction path in any device structure where a depletion region can be formed when appropriately biased. This technique is suitable not only to the study of bulk semiconductor materials but also to actual device structures such as p–n diodes, Schottky barrier diodes, or any devices that contain such basic structures. Examples would be bipolar junction transistors, field-effect transistors, or derivatives thereof.

Emission Rate

Consider an n-type semiconductor with only a single deep electron trapping level within the band gap in addition to the donor level as shown in Figure 1. Assume also that the trapping level is located at an energy level E_T from the conduction band edge, E_C. The donor level is indicated by a shallow energy level E_D that is closer to the conduction band edge.

The probability that an electron is captured by the deep electron trap is given by

$$c_n = n v_{th} \sigma_n \tag{1}$$

where n is the electron concentration, v_{th} is the mean thermal velocity, and σ_n is the electron capture cross-section. The rate of capture of an electron depends not only on the capture probability, c_n, but also on the

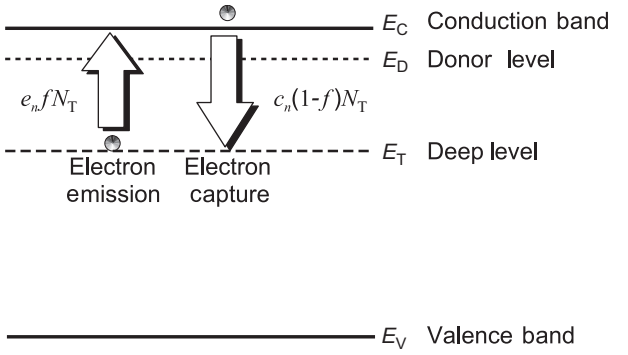

Figure 1. Electron transitions between trapping level and conduction band.

availability of a vacant trap as measured by the concentration of unoccupied traps, N_T°. The electron capture rate can therefore be expressed as

$$\frac{dc_n}{dt} = c_n N_T^\circ = n v_{th} \sigma_n N_T^\circ \tag{2}$$

The concentration of unoccupied traps N_T° can be written in terms of the probability that a given trap out of the total concentration of traps, N_T, is empty, that is:

$$N_T^\circ = (1-f)N_T \tag{3}$$

where $(1-f)$ is the probability that a trap is vacant and f is the Fermi–Dirac factor.

Therefore, the rate of electron capture can now be written as

$$\frac{dc_n}{dt} = n v_{th} \sigma_n (1-f) N_T \tag{4}$$

The rate of electrons escaping from the traps is dependent on both the emission rate e_n and the concentration of occupied traps, N_T^-. Therefore, the electron detrapping rate can be written as

$$\frac{de_n}{dt} = e_n N_T^- \tag{5}$$

The concentration of occupied traps N_T^- can also be expressed in terms of the probability that a fraction of the total concentration of traps, N_T, is filled. This probability is represented by the Fermi–Dirac factor f. Therefore:

$$\frac{de_n}{dt} = e_n f N_T \tag{6}$$

According to the principle of detailed balance, the rate of electron capture should balance the rate of electron emission. This means that the concentration of free electrons should remain constant, or

$$\frac{dn}{dt} = 0 = e_n f N_T - n v_{th} \sigma_n (1-f) N_T \tag{7}$$

Therefore:

$$e_n f N_T = n v_{th} \sigma_n (1-f) N_T \tag{8}$$

or

$$e_n = n v_{th} \sigma_n \frac{1-f}{f} \tag{9}$$

The Fermi–Dirac factor f is given by

$$f = \frac{1}{1 + (1/g) e^{(E_T - E_F)/kT}} \tag{10}$$

where g is the degeneracy factor. The degeneracy factor takes into consideration the fact that a given energy level can be occupied by an electron of either spin or no electron at all.

The free electron concentration, n, is given by

$$n = N_C \, e^{(E_F - E_C)/kT} \tag{11}$$

where N_C is the density of states in the conduction band.

Substituting for f and n, the electron emission rate, e_n, can be written as

$$e_n = \frac{N_C v_{th} \sigma_n}{g} e^{-(E_C - E_T)/kT} \tag{12}$$

By using the following relationships:

$$N_C = \left[\frac{2\pi m_e^* kT}{h^2}\right]^{3/2} \tag{13}$$

where m_e^* is the electron effective mass, k is the Boltzmann constant, T is the temperature, and h is the Planck constant, and

$$v_{th} = \sqrt{\frac{8kT}{\pi m_e^*}} \tag{14}$$

the equation for the electron emission rate, e_n, can be expressed as

$$e_n = \frac{16\pi m_e^* k^2 \sigma_n T^2}{g h^3} e^{-(E_C - E_T)/kT} \tag{15}$$

By taking the natural logarithm, we arrive at the following equation:

$$\ln \frac{e_n}{T^2} = \ln\left[\frac{16\pi m_e^* k^2 \sigma_n}{g h^3}\right] - \frac{E_C - E_T}{kT} \tag{16}$$

It can been seen from this equation that the slope of the Arrhenius plot of $\ln(e_n/T^2)$ against $1/T$ gives the activation energy of the electron trap relative to the conduction band edge, $(E_C - E_T)$. The y-intercept of this plot gives the capture cross-section σ_n of the electron trap. If the root-mean-square value of the thermal velocity is used instead of Equation 14, then $v_{th} = (3kT/m_e^*)^{1/2}$. This will result in a small variation in the value of the capture cross section, the difference of which is small compared to the experimental errors.

The next task is to determine the emission rate, en, at a range of temperatures so that an Arrhenius plot can be made.

Junction Capacitance Transient

We consider, for simplicity, a Schottky barrier diode formed on an n-type semiconductor. The energy band diagram of a Schottky barrier diode under different bias conditions is shown in Figure 2. Figure 2a shows the diode in the reverse-biased condition. In the space charge or depletion region, denoted by the shaded area of the figure, all the electron traps above the Fermi level are ionized or empty. In Figure 2b, the reverse bias is reduced by introducing a short pulse (one can also apply a short forward bias pulse), thus reducing the width of the depletion region. By doing so, the electrons are now allowed to be captured at the traps, thus filling up the traps. Figure 2c shows that when the bias is returned to the original reverse bias condition, the electrons begin to be thermally excited or emitted to the conduction band by absorbing thermal energy. The capacitance of the junction will vary in response to changes in the width, w_d, of the space charge region according to

$$C = \frac{\varepsilon A}{w_d} \tag{17}$$

where ε is the permittivity of the semiconductor and A is the surface area of the gate contact.

The width, w_d, is in turn dependent on the concentration of charged states or electron trapping centers in the material as well as the applied bias across the junction as shown by the following equation:

$$w_d = \sqrt{\frac{2\varepsilon\left(V_{bi} + V_r - \frac{kT}{q}\right)}{q\left(N_D^+ + N_T\right)}} \tag{18}$$

where V_{bi} is the built-in potential of the barrier, V_r is the applied reverse bias, q is the electronic charge, and N_D^+ is the concentration of ionized donor centers.

If we assume that the falling edge of the pulse coincides with time $t = 0$, we can denote the capacitance at time $t = 0$ as $C(0)$, and that at a sufficiently long delay ($t = \infty$) after the end of the pulse as $C(\infty)$. The capacitance $C(\infty)$ is actually the capacitance of the junction under quiescent reverse bias condition, C_o. It is commonly accepted, within certain restrictions (Look, 1989), that the difference in the capacitance, $\Delta C(0) = C(0) - C(\infty)$, is related to the concentration of the electron traps by

$$\frac{\Delta C(0)}{C(\infty)} \cong \frac{N_T}{2N_D} \tag{19}$$

where $N_T \ll N_D$; N_D is the net dopant concentration and N_T is the trap concentration.

The time variation of the capacitance following the applied bias pulse is shown in Figure 3. As the trapped electrons emit to the conduction band following the termination of the bias pulse, the capacitance of the junction will decay exponentially with a time constant τ_n according to the following equation:

$$C(t) = C_o\left[1 - N\, e^{-t/\tau_n}\right] \tag{20a}$$

where

$$N = \frac{N_T}{2N_D} \tag{20b}$$

The decaying time constant of the capacitance transient is related to the emission rate of the trapped electrons according to

$$e_n = \frac{1}{\tau_n} \tag{21}$$

Equation 20a can therefore be written as

$$C(t) = C_o\left[1 - N\, e^{-e_n t}\right] \tag{22}$$

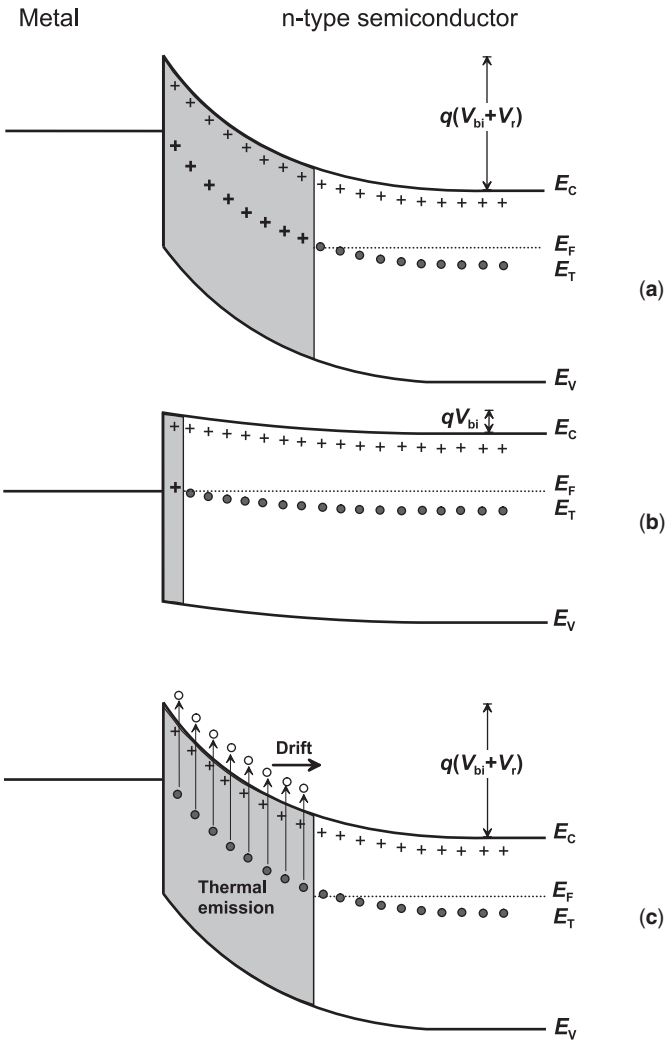

Figure 2. Energy band diagrams for a diode under: (**a**) reverse-bias; (**b**) reduced bias pulse; and (**c**) restored reverse-bias.

Determination of the Emission Rate

The fundamental objective of DLTS is to determine the emission rate from the capacitance transient as given by

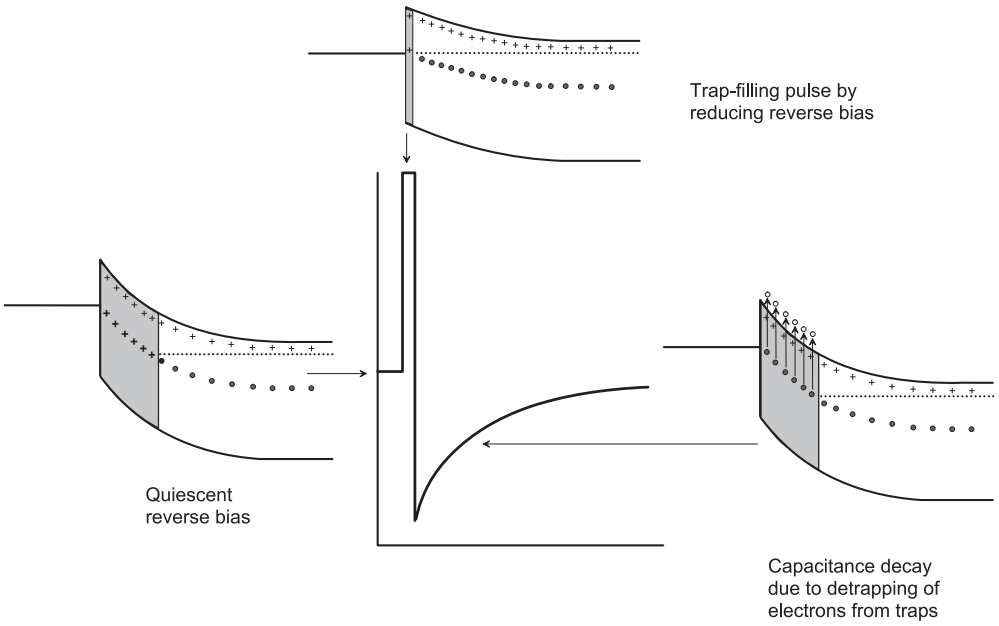

Figure 3. Time variation of junction capacitance during different biasing conditions for majority carrier trap.

Equation 22. This problem is trivial if there is only one trapping center with the capacitance transient following a single component exponential decay function. The problem is more complicated if there are multiple trapping centers with different emission rates thereby producing a multicomponent exponential capacitance decay as given by the following equations:

$$C(t) = C_{\mathrm{o}}\left[1 - \sum_{\alpha} N_{\alpha} e^{-t/\tau_{n\alpha}}\right] \tag{23}$$

or

$$C(t) = C_{\mathrm{o}}\left[1 - \sum_{\alpha} N_{\alpha} e^{-e_{n\alpha} t}\right] \tag{24}$$

where $N_{\alpha} = N_{\mathrm{T}\alpha}/2N_{\mathrm{D}}$, $\tau_{n\alpha}$ and $e_{n\alpha}$ are the decay time constant and the emission rate, respectively, for the decay component, α.

Multicomponent exponential decay is commonly encountered in many fields. The problem of determining the decay time constants from a multicomponent exponential decay signal has been studied for decades, particularly for situations that involve significant noise level (Gafni et al., 1975; Smith et al., 1976; Provencher, 1982; Halvorson, 1992; Marco et al., 1995; Kryzhniy, 2004). Most analytical methods involve numerical analysis and significant computing time. However, with current desktop computing power, this task is no longer an impediment. These numerical techniques require that the complete transient at each temperature be recorded. Again, this task of acquiring a complete transient is now easy to implement with economical analog-to-digital converter boards.

The different analytical methods to determine the decay time constants can be adopted to analyze DLTS data. The main objective for the various techniques is the need to determine the trapping parameters of multiple traps with less ambiguity as well as to provide a spectroscopic or spectral plot that can be used as a signature for a particular defect. The popular conventional rate window technique, Fourier transform (Ikeda and Takaoka, 1982; Kirchner et al., 1981; Weiss and Kassing, 1988), and the Laplace transform (Nolte and Haller, 1987; Dobaczewski et al., 2004) methods will be discussed here.

Rate Window Technique

The rate window technique is the original classical DLTS technique, which remains the fundamental technique that can be implemented instrumentally. This technique is still useful because it provides fast, real-time monitoring of a DLTS experiment. Real-time data display during a DLTS experiment allows for detection of any abnormal behavior and helps to determine whether to proceed or to abort an experiment when a problem arises.

If the decaying capacitance transient is measured at two different time delays t_1 and t_2 from the termination of the bias pulse, then the difference in the capacitances will be given by

$$\begin{aligned} S = \Delta C &= C(t_1) - C(t_2) \\ &= C_{\mathrm{o}} N\left(-e^{-e_n t_1} + e^{-e_n t_2}\right) \end{aligned} \tag{25}$$

The capacitance difference, S, is the DLTS signal.

In the case of an n-type material, it can be seen from Figure 4 that as the temperature changes, the time constant of the decaying transient also changes. The time constant at low temperature is longer reflecting the low emission rate of the trapped electrons due to inadequate thermal energy necessary for the electrons to escape. As the temperature of the sample increases, the time constant becomes shorter corresponding to a faster rate of emission of the trapped electrons since there is an increasing availability of thermal energy required for excitation into the conduction band.

By monitoring the DLTS signal S, which is the difference in the capacitances at two different delay times, as a function of temperature, it can be seen that at a low temperature ($T \ll T_m$) and at high temperature ($T \gg T_m$), the signal is very small. However, at an intermediate temperature T_m the signal will go through a maximum value. At this temperature T_m the variation of the DLTS signal S with temperature can be described by

$$\frac{dS}{dT} = \frac{dS}{de_n} \times \frac{de_n}{dT} = 0 \tag{26}$$

Therefore:

$$\frac{dS}{de_n} = C_o N\left(t_1\, e^{-e_n t_1} - t_2\, e^{-e_n t_2}\right) = 0 \tag{27}$$

which gives

$$e_n = \frac{\ln(t_2/t_1)}{t_2 - t_1} \tag{28}$$

This equation means that if the time delays t_2 and t_1 are known, then at the temperature T_m at which the signal S is a maximum, the emission rate of the trapped electron, valid only for that particular temperature T_m, can be calculated according to Equation 28. By varying t_2 and t_1 but keeping the ratio t_2/t_1 constant (thus changing to a different value of e_n), and repeating the temperature scan, a different curve will be obtained with the signal S peaking at a different temperature T_m. By repeating the procedure for several values of e_n, and obtaining the corresponding set of temperatures T_m, an Arrhenius plot of $\ln(e_n/T^2)$ against $1/T$ can be graphed to give the activation energy and the capture cross-section of the electron traps.

The efficiency of the classical DLTS lies in the way in which the trapping parameters (activation energy and capture cross-section) are obtained experimentally. In the experiment, the capacitance transients are sampled at two different instants of time t_1 and t_2 from the end of the bias pulse. The expression $(t_2 - t_1)/\ln(t_2/t_1)$ can be considered as a time window. The reciprocal of this time window is the rate window. In essence, as the temperature changes, the emission rate of the carriers also varies until a temperature is reached at which the emission rate matches the rate window set by t_2 and t_1.

Figure 5 shows an example of how an Arrhenius plot is made from the DLTS signals.

Fourier Transform DLTS

The Fourier transform method is based on the principle that a periodic signal can be described by a series of sine and cosine functions. For a decaying transient, the Fourier transform of the signal is given by

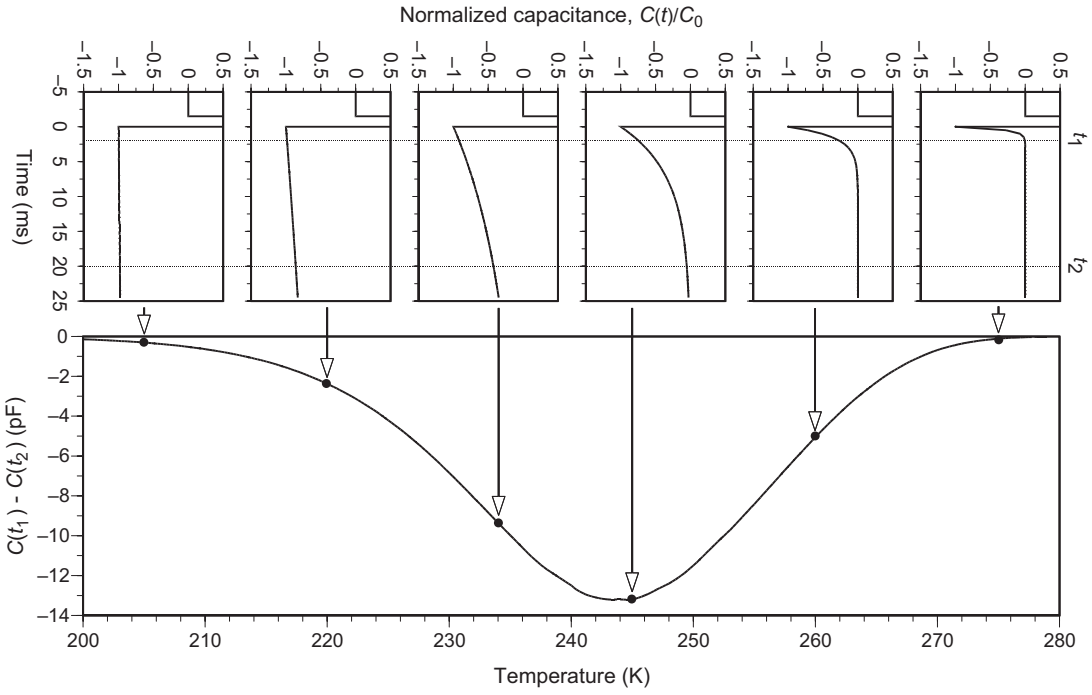

Figure 4. Temperature dependence of time constant of capacitance transient.

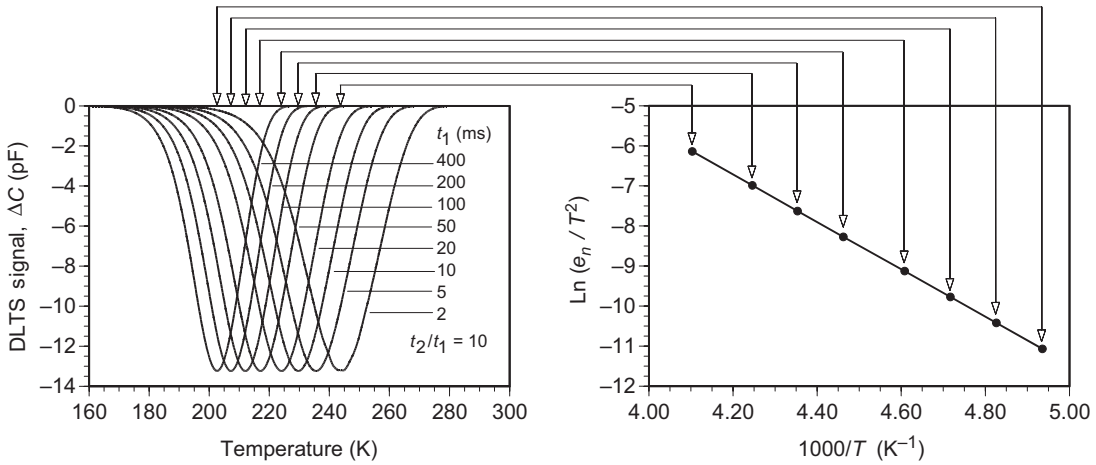

Figure 5. Deriving an Arrhenius plot from DLTS signals. The DLTS signals are measured at different values of t_1 with $t_2/t_1 = 10$. The emission rates, determined using Equation 28, and the temperatures corresponding to the DLTS peaks are then used to obtain the Arrhenius plot.

$$C(t) = \frac{a_o}{2} + \sum_{\alpha=1}(a_\alpha \cos \alpha\omega t + b_\alpha \sin \alpha\omega t) \tag{29}$$

where $\omega = 2\pi/t_p$, with t_p being the period or time window, and a_o, a_α, and b_α are the Fourier coefficients. The period, t_p, is related to the sampling interval, Δt, by $t_p =$ (number of sampling interval) $\times \Delta t$, or $(M-1)\Delta t$, where M is the number of samples in each transient. If t_o is the time coinciding with the falling edge of the filling pulse, then the Fourier coefficients can be written as follows:

$$a_o = 2\left(C_o - \frac{A}{e_n t_p}\right) \tag{30a}$$

$$a_\alpha = 2e_n t_p A/U_\alpha \tag{30b}$$

$$b_\alpha = 2\alpha\omega t_p A/U_\alpha \tag{30c}$$

where

$$U_\alpha = t_p^2\left(e_n^2 + \alpha^2\omega^2\right) \tag{31}$$

$$A = C_o N e^{-e_n t_o}\left(1 - e^{-e_n t_p}\right) \tag{32}$$

Since the cosine and sine functions are actually damped oscillations, the higher order Fourier coefficients, a_α and b_α, decrease rapidly, and only the lower orders ($\alpha = 1$, 2, or 3) are used. The Fourier coefficients are functions of the emission rate e_n. The emission rate, e_n, can be determined using different ratios of the Fourier coefficients, such as a_α/b_α, a_α/a_β, or b_α/b_β, where $\alpha \neq \beta$. The most convenient way is to use the ratio of the Fourier coefficients of the same order, that is:

$$e_n = \alpha\omega\frac{a_\alpha}{b_\alpha} \tag{33}$$

A plot of either of the coefficients, that is, a_α or b_α, as function of temperature, T, will show a peak if there is a trap, similar to a conventional rate window DLTS plot. The height of the peak is related to the concentration of the trap. The emission rate calculated from a transient at a temperature, T, is then used together with T to calculate the trapping parameters using the Arrhenius plot of $\ln(e_n/T^2)$ against $1/T$.

In the case of multiple traps with small differences in the values of the trapping parameters, the plot of the temperature dependence of the Fourier coefficients may show overlapping peaks. In this case, one can use the ratio of the a coefficient, that is, a_1/a_2, to determine the emission rate for one trap and the ratio of the b coefficient, that is, b_1/b_2, for the other trap (Weiss and Kassing, 1988).

The Fourier technique provides several advantages compared to conventional DLTS. Unlike conventional DLTS, whose accuracy depends largely on an accurate determination of the peak temperature, T_m, from the temperature scan, the emission rate can be determined from the transient at each temperature T. A complete temperature scan in the Fourier DLTS can provide more data points, and thus more accuracy, for the Arrhenius plot. Another advantage is that the pre-exponential coefficient, or the amplitude, of the exponential transient is determined separately from the emission rate, thus removing any potential error from the temperature dependence of the amplitude. If precautions are taken as discussed by Weiss and Kassing (1988), Fourier DLTS can provide higher energy resolution than conventional DLTS.

Laplace Transform DLTS

The use of Laplace transform to calculate the time constant of a multicomponent exponential transient is well known. This method is now commonly employed in the analysis of DLTS data. Due to the time-consuming numerical iteration needed to analyze individual transient, this analysis is done only after the experiment. There are two approaches in using Laplace transform to analyze exponential decay function. One is to use the forward Laplace transform and the other is to use the

inverse Laplace transform.The Laplace transform of a function, $f(t)$, can be written as

$$L(s) = \int_0^\infty f(t)e^{-st}\,dt \tag{34}$$

where s is the transform space.

If $f(t)$ is an exponential decay transient of the form

$$f(t) = A\,\mathrm{e}^{-e_n t} \tag{35}$$

where A is the amplitude and e_n is the emission rate, the Laplace transform of $f(t)$ is

$$L(s) = \int_0^\infty A\,\mathrm{e}^{-e_n t}\,\mathrm{e}^{-st}\,dt \tag{36}$$

The solution of the Laplace transform of an exponential function is exact and is given as

$$L(s) = \frac{A}{s+e_n} \tag{37}$$

The problem is to fit the solution (37) to the real-time exponential transient data to obtain the amplitude A and the emission rate e_n. One method to solve for A and e_n is to use Padé–Laplace approximation (Hellen, 2005).

Another Laplace transform method is to use the inverse Laplace transform. The inverse Laplace transform method treats the experimental decay transient as the Laplace transform of a function in the transform space, s. The domain s is, conveniently, the emission rate, e_n.

If $f(t)$, which is the exponential decay transient in the real-time domain, is the Laplace transform of $g(s)$, to be referred to as the spectral function, then $f(t)$ can be written as

$$f(t) = \int_0^\infty g(s)\mathrm{e}^{-st}\,ds \tag{38}$$

The spectral function, $g(s)$, is therefore the inverse Laplace transform of $f(t)$. If $f(t)$ follows an exponential decay function of the form

$$f(t) = \sum_i C_i\,\mathrm{e}^{-e_{ni}t} \tag{39}$$

then $g(s)$ is a delta function of the form

$$g(s) = \sum_i C_i\delta[s-e_{ni}] \tag{40}$$

Therefore, a plot of $g(s)$ versus s will produce a peak when $s = e_n$. A plot of $g(s)$ versus s (or e_n) at a particular temperature T provides a spectral plot that can be used as a defect signature. The area of the peak is proportional to the trap concentration.

Figure 6 illustrates the inverse Laplace transform of a double exponential decay transient. As shown in Figure 4, as the temperature changes, the decay time constant (or the emission rate) will also change. The inverse Laplace transform results would show several peaks at different temperatures as shown in Figure 7. To illustrate the use of inverse Laplace transform, the absolute values of some of the transients shown in Figure 4 are used to generate the inverse Laplace transform results shown in Figure 7.

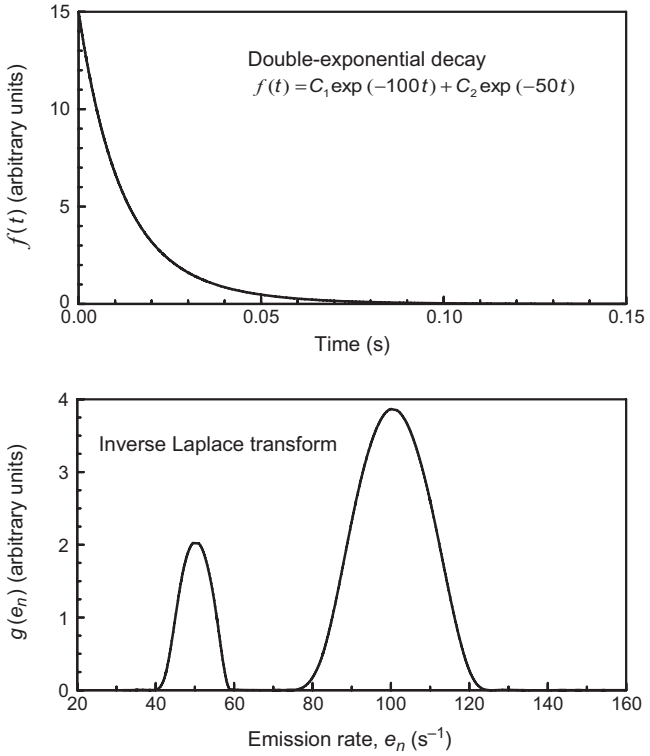

Figure 6. Illustration of the inverse Laplace transform of a double exponential decay function.

The activation energy and capture cross-section are calculated by using the Arrhenius plot of the different emission rates obtained at different temperatures, similar to the procedure used for the rate window

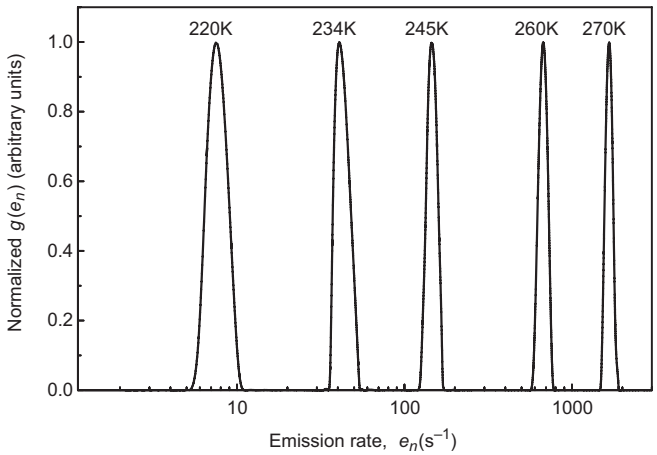

Figure 7. Illustration of the inverse Laplace transform of capacitance transients at different temperatures.

technique. However, there is no need to find the peak temperature, T_m, as in conventional DLTS because the averaged transient at every temperature can be used.

The main problem in the use of inverse Laplace transform is that Equation 38 is an ill-posed or ill-conditioned equation with no exact solution. Regularization techniques must be used to solve Equation 38 (Provencher, 1982; Kryzhniy, 2004). Several inverse Laplace transform algorithms are available in the public domain, the most popular of which is CONTIN, which is a regularization method to handle noisy experimental data. A simplified version of CONTIN, written as MATLAB script, was used to generate the plots of Figures 6 and 7. It should be noted that numerical methods, in general, can provide misleading results if not properly used. The regularization algorithms to solve the inverse Laplace transform of real data according to Equation 38 are susceptible to noise and can be unstable. The successful convergence of the iterative procedure depends very much on initial values. Several computational runs need to be done to check for accuracy. The results also depend on the algorithms and it is therefore recommended that several different programs be used in order to obtain consistent results.

The main advantage of using numerical techniques, such as Fourier or Laplace transforms, is that the determination of the emission rate for a given temperature is more well defined, or less ambiguous. The disadvantage is that the postexperiment data analysis is time consuming because of the numerical procedure needed to fit the equation to the actual transient. In order to reduce noise, multiple transients should be recorded and averaged, which means that a DLTS scan can involve literally thousands of transients.

Interface States

Interface states are defect levels at the interface between a semiconductor and an insulator in a metal–insulator–semiconductor (MIS) structure, which includes the metal–oxide–semiconductor (MOS) structure. Interface states affect the performance of MIS- or MOS-based field-effect transistors (FET). The quality of a metal–insulator–semiconductor interface is defined by the interface states density, D_{it}, which is a function of the energy level E. D_{it} is usually plotted as a function of E. DLTS can be used to characterize the D_{it} in MIS- or MOS-based FET structures (Yamasaki et al., 1979; Johnson, 1982). DLTS method has been shown to be more reliable than the conventional Terman method to calculate D_{it} (Rosencher and Bois, 1982).

The D_{it} can be calculated from DLTS signal, S, using the following equation:

$$D_{it}(E) = \frac{\varepsilon C_{ox} N_D S}{C_o^3 kT \ln\left(\frac{t_2}{t_1}\right)} \tag{41}$$

where ε is the permittivity of the semiconductor, C_{ox} is the oxide capacitance, N_D is the substrate doping concentration, S is the DLTS signal ($C(t_1) - C(t_2)$), C_o is the capacitance of the MIS structure during quiescent reverse bias, k is the Boltzmann constant, and T is the temperature.

The energy level, E, can be calculated from the peak location of the DLTS signal as follows:

$$E = E_C - kT \ln\left[\frac{\sigma_n(E)\upsilon_{th}N_C}{e_n}\right] \tag{42}$$

PRACTICAL ASPECTS OF DLTS INSTRUMENTATION AND METHOD AUTOMATION

The first DLTS experimental setup was reported by Lang (1974) and is popularly known as the boxcar technique. A block diagram of a basic DLTS spectrometer using the boxcar technique is shown in Figure 8. The high-frequency capacitance meter measures the capacitance across the junction device and typically has a 1 MHz test frequency. A pulse generator with variable pulse width

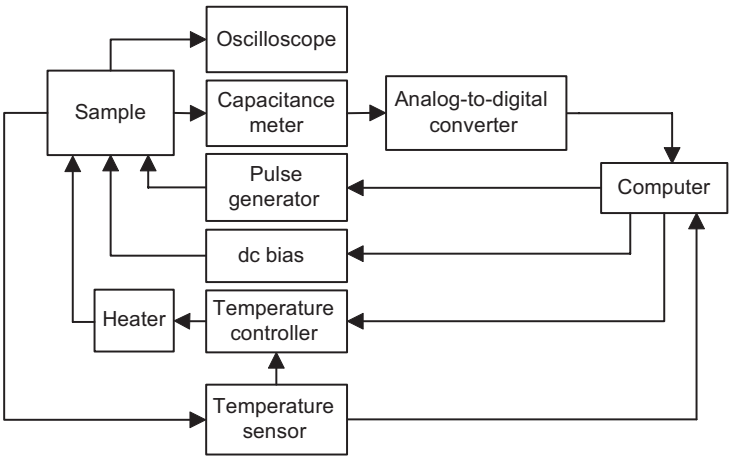

Figure 8. DLTS spectrometer using the boxcar technique.

and pulse height as well as a variable dc offset bias is required to provide a steady-state or quiescent reverse bias as well as providing the trap-filling pulse. A standard dc power supply can also be used instead of the dc offset bias of the pulse generator. In fact, a standard dc power supply may be able to give a wider range of reverse bias. An analog-to-digital converter is needed to digitize the analog output of the capacitance meter. A fast digital voltmeter with digital output connected to a computer can also be used for this purpose. It is also helpful to have an oscilloscope to visually monitor the capacitance transient. Poor or degraded contacts on the sample can give noisy or spurious signal and an oscilloscope is a good diagnostic tool for detecting any problem. A computer is necessary for data collection, analysis, and archival. In the past, an analog x–y pen recorder was commonly used but such recording device does not allow for data manipulation, analysis, or storage. The temperature of the sample must be variable. A wide temperature range is required in order to detect the trapping levels from near the energy band edges to the middle of the band gap. A temperature range of about 77–380 K would be sufficient to detect trapping levels from about 0.1 to about 0.85 eV for most semiconductors. A higher temperature up to about 570 K would be needed for wide band gap semiconductors such as GaN or SiC. Since the sample temperature needs to be as low as 77 K, a mechanical pump and a vacuum sample chamber or cryostat would be needed to prevent ambient moisture from condensing on the sample. Although a temperature controller would be helpful for precise temperature control, it is not a real necessity if the sample temperature can be slowly varied at a rate small enough to avoid any temperature lag between the temperature sensor and the sample.

The DLTS system shown in Figure 8 is more flexible in the way the data can be processed. The system would allow for the complete decay transient to be digitized and the rate window technique can then be applied by writing a simple program to analyze the stored data files after the experiment. However, besides saving the complete data for later analysis, it is also advisable that the DLTS signal be plotted in real time on the computer by simply plotting the difference between two capacitance values taken from the data file at two fixed delay times against the sample temperature at which the data were measured. In this manner, it is possible to see immediately whether there is any peak in the DLTS curve. In the event that there is no peak observed as the temperature is scanned, the operator can choose to terminate the experiment early without wasting much time. The operator should consider different choices of delay times and biasing conditions in order to obtain an optimum DLTS curve. A typical experiment would consist of gradually heating the sample from the low end of the temperature range to the high end and recording the capacitance transient at an appropriate temperature interval. If the complete transient is recorded, then only a single temperature scan is needed. Previously, DLTS temperature scans have to be repeated several times because only a single fixed rate window can be applied at each scan. This is tedious and sometimes detrimental to the sample. The automated approach described here is akin to a multichannel approach where all the rate windows can be applied simultaneously. Obviously, if the complete transient can be digitized using the system in Figure 8, then it is also possible, especially with the power of present desktop personal computers, to extract the time constants numerically by nonlinear curve fitting of each transient.

An alternative method that employs an instrumental approach, as opposed to the software technique described previously, to extract the DLTS curves is shown in Figure 9. This version can be used to monitor the experiment by providing a real-time view of the data. In this method, an electronic circuit is used to perform the subtraction of the capacitance values to give the DLTS signal. The circuit essentially has two sample-and-hold amplifiers, each of which is separately triggered to hold the analog voltage corresponding to a capacitance value at a preset time delay from the end

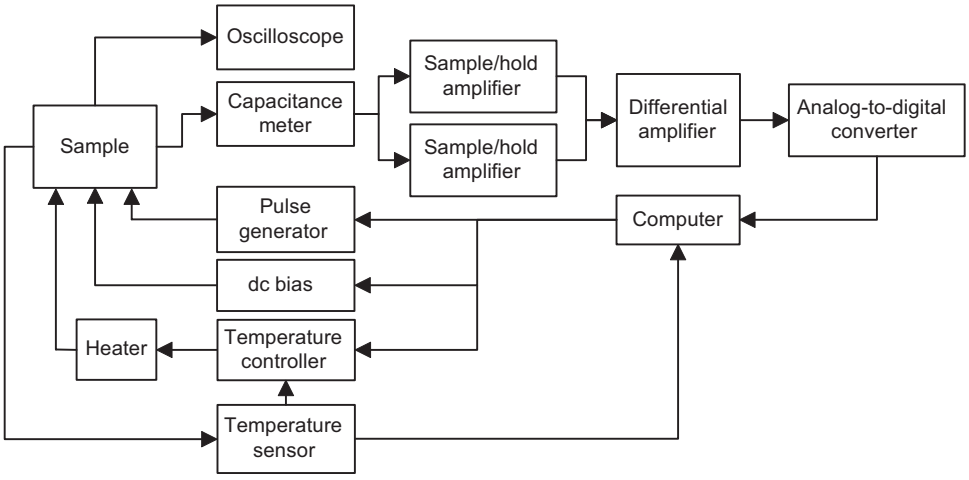

Figure 9. DLTS spectrometer using the sample-and-hold amplifier technique.

of the bias pulse. Since there are two sample-and-hold amplifiers, therefore two analog voltages corresponding to the capacitances at two different parts of the capacitance transient are stored. The outputs from the sample-and-hold amplifiers are then fed into a differential amplifier to give an analog signal that is proportional to the difference between the two capacitances. This analog signal is the DLTS signal and can be further amplified and recorded by a digital voltmeter or analog-to-digital converter and then transferred to a computer. Each circuit can only provide one rate window or a single DLTS curve. The circuit can be built as a module, and by using several modules together, several DLTS curves corresponding to different rate windows can be obtained at the same time in a single temperature scan.

The elegance of the original DLTS lies in the instrumental extraction of the time constant from the capacitance decay without the use of numerical analysis. Other instrumental methods (Kimerling, 1976; Day et al., 1979; Auret, 1986; Miller et al., 1975, 1977) are also available to measure the rate window. A standard test method, based on the rate window technique, for using the DLTS technique has also been published (ASTM F978-90, 1993). Since the first introduction of DLTS, many variations of the experiment have also been introduced besides the Fourier and Laplace transforms methods described above. Examples of such variations are electron beam scanning DLTS (Petroff and Lang, 1977), photoexcited DLTS (Mitonneau et al., 1977; Brunwin et al., 1979; Takikawa and Ikoma, 1980), current or conductance DLTS (Wessels, 1976; Borsuk and Swanson, 1980), constant-capacitance DLTS (Goto et al., 1973; Johnson, 1982), lock-in amplifier DLTS (Miller et al., 1975), and isothermal DLTS (Okushi and Tokumaru, 1980).

DATA ANALYSIS

For conventional DLTS, for each value of the emission rate, e_n, corresponding to a set of t_1 and t_2, a graph of DLTS signal as a function of temperature is plotted. The emission rate, e_n, is related to t_1 and t_2 according to Equation 28. The temperature, T_m, at which the peak occurs is recorded. The graphing procedure is repeated for several emission rates that are obtained experimentally by changing t_1 and t_2. For each value of e_n, there is a corresponding value of T_m. An Arrhenius plot of $\ln(e_n/T_m^2)$ against $1/T_m$ is then plotted. From Equation 16, it can be seen that the slope of the linear graph will give the activation energy and the y-intercept will give the capture cross-section. The maximum DLTS signal gives the concentration of the defects according to Equation 19.

For Fourier transform DLTS, the emission rate, e_n, is obtained for each temperature T. An Arrhenius plot is then obtained as described above. A plot of the Fourier coefficients as function of temperature is used as defect signature. It is optional whether to use the peak temperatures from the temperature scan to calculate the emission rate from the Fourier coefficients of the transients or to calculate the emission rate for a range of temperature, not necessary at the peak temperatures.

For Laplace transform method, the emission rates for a range of temperature are obtained by inverse Laplace transform. An Arrhenius plot is then used to obtain the trapping parameters. A plot of the spectral function as function of emission rate is used as the defect signature.

SAMPLE PREPARATION

A sample for DLTS measurement must contain a voltage-controlled depletion region. Schottky barrier diodes and p–n diodes are suitable samples. A Schottky barrier diode is the most convenient type of sample. This diode is simply a metal placed in contact with a semiconductor to form an energy barrier or Schottky barrier at the interface. The selected metal must have a sufficiently high Schottky energy barrier to produce a rectifying contact with low leakage current. The surface of the semiconductor must be clean because surface impurities can reduce the effective barrier height and increase current leakage. The metal film, or gate contact, can be deposited on the semiconductor by vacuum evaporation, sputtering, or chemical vapor deposition. For standard capacitance–voltage measurement, a mercury probe in contact with the semiconductor is adequate to form a Schottky barrier diode. However, this contacting technique is not advisable in DLTS because the temperature of the sample has to be varied over a wide range. Schottky barrier diodes are easily formed on semiconductors of low doping concentration. They tend to exhibit large leakage current with increasing doping concentration. DLTS measurement does not work well with leaky diodes.

A p–n diode is made by forming a junction between an n- and a p-type material. Due to the fact that the interface between the n- and p-type materials must be clean, this type of diode is usually formed by controlled introduction of dopants either by alloying, diffusion, and ion implantation or during epitaxial growth.

Both Schottky and p–n diodes also need low-resistivity ohmic contacts to allow for electrical connections to be made between the semiconductors and the electronic equipment. It is easier to form an ohmic contact on a semiconductor of high doping concentration ($\sim 10^{18}\,\mathrm{cm}^{-3}$) than one with a low doping concentration because the narrow width of the Schottky barrier formed by a metal on a highly doped semiconductor encourages current conduction by carrier tunneling through the thin barrier. Ohmic contact formation on highly doped material may or may not require alloy formation by thermal annealing. In some semiconductors, it is possible to get some metals to form good ohmic contacts even when the semiconductors have a low carrier concentration of about 10^{14}–$10^{15}\,\mathrm{cm}^{-3}$. The formation of ohmic contacts in such cases would invariably include alloy formation through rapid thermal annealing of the metal–semiconductor interface. A common sample configuration is one where the semicon-

ductor material of interest is grown on a highly doped or low-resistivity substrate of the same material. Schottky or p–n diodes are formed on the top surface while ohmic contact is made at the back of the low-resistivity substrate.

In DLTS experiments using Schottky diodes, it is possible to avoid ohmic contact problems by making the back contact on the substrate larger than the cross-sectional area of the depletion region of the sample. In practice, the size of the gate contact is made smaller than the back contact. In this configuration, the larger back contact will have a larger capacitance than that of the depletion region. The resultant capacitance will be largely that of the depletion region, which is the region of interest.

It is often necessary for the diode cross-sectional area to be known so that it can be used in data analysis. In the case of the Schottky diodes, diode structures of the required size can be made by vacuum evaporation or sputtering of metal through a shadow mask containing holes of the required dimensions. Alternatively, the metal film can be patterned through photolithography and etching to produce Schottky diode structures of different sizes. p–n junction diodes can only be patterned through photolithography and etching.

Since any sample containing a bias-controlled depletion region can be used for DLTS measurement, this technique can be applied not only to individual discrete diodes but also to junction diodes found in devices such as bipolar and field-effect transistors. DLTS can therefore be used for analysis of actual transistors. The potential applications of DLTS as a diagnostics tool for actual devices make it a powerful technique for understanding the role of electrically active defects in device performance and reliability.

PROBLEMS

The shortcoming of DLTS, or any method that requires a depletion region, is that it is not effective for high-resistivity materials due to the problems involved in obtaining suitable junctions on such materials. Furthermore, because of the low concentration of free carriers in such materials, an application of a reverse bias may cause the whole sample to be depleted. This shortcoming leads to the introduction of photoinduced current transient spectroscopy (PICTS or PITS) (Hurtes et al., 1978; Fairman et al., 1979; Yoshie and Kamihara, 1983a,b, 1985; Look, 1983; Tin et al., 1987). PICTS employs the same gating technique but uses a light pulse instead of a voltage pulse, and does not require a depletion region to be formed.

The interpretation of DLTS curves is susceptible to errors. One of the precautions that requires consideration is that if the circuit impedance is high (which could be due to high sample resistivity or poor contacts), it will cause a disproportionately large time constant that is due to the increase in the *RC* time constant of the measurement setup and not due to a very deep trapping center. In such cases, the DLTS curves would lack sharp or well-defined peaks. Such samples are commonly encountered in studies of irradiation effects in semiconductors (Lang, 1977; Tin et al., 1991a,b). A broad peak can also be indicative of a range of closely spaced energy levels producing capacitance transients with multiexponential characteristics. In certain cases, it is possible to separate the closely spaced peaks by using large (t_2/t_1) ratio or large values of $(t_2 - t_1)$. In the use of DLTS for depth profiling of defects, the effect of fringing capacitance around the gate contact also needs consideration.

A featureless or flat DLTS curve does not mean an absence of trapping centers. Experiments with different quiescent bias and pulse height settings should be tried to provide an indication as to the optimum parameters to be used for subsequent high-resolution scan.

Traps with very large or very small capture cross-sections are not easily detected (Miller et al., 1977). Different experimental conditions and samples should be used in order to provide as much detail of the defect structure as possible.

The steady-state capacitance of the sample changes with temperature. This causes the dc level to shift with temperature. A baseline restoring circuit would resolve this problem (Miller et al., 1975). Another solution to this problem is to reduce the rate of temperature increase to ensure that the sample temperature does not change appreciably while the capacitance is relaxing to its steady-state value after each bias pulse.

During the peak of each bias pulse, the capacitance meter will show an overload. The capacitance meter should have a fast pulse overload recovery in order to measure fast transients.

Data acquisition should only be initiated after the meter has recovered from overload.

SUMMARY

The defect structure in a semiconductor consists of a group of well-defined carrier trapping levels. DLTS is an effective method to characterize the defect structure of a semiconductor. Since different semiconductors would have different combinations of defect levels with different activation energies and capture cross-sections, a DLTS curve taken at a known rate window can be used as a defect signature that is characteristic of the material. A knowledge of the various defect levels in a semiconductor is important to understanding the electronic properties of the material. DLTS curves do not describe the exact nature or the chemical origin of the defects. DLTS data require a proper and informed interpretation. They are best used in conjunction with other appropriate methods described in this book.

BIBLIOGRAPHY

"Deep-Level Transient Spectroscopy" in *Characterization of Materials*, 1st ed., Vol. 1, pp. 418–427, by Chin-Che Tin, Auburn University, Auburn, Alabama; Published online: October 15, 2002; DOI: 10.1002/0471266965.com036.

LITERATURE CITED

ASTM F978-90. 1993. Standard test method for characterizing semiconductor deep levels by transient capacitance techniques. *In* 1993 *Annual Book of ASTM Standards*, Vol. 10.05, pp. 534–541. ASTM, Philadelphia.

Auret, F. D. 1986. Considerations for capacitance DLTS measurements using a lock-in amplifier. *Rev. Sci. Instrum.* 57:1597–1603.

Borsuk, J. A. and Swanson, R. M. 1980. Current transient spectroscopy: A high-sensitivity DLTS system. *IEEE Trans. Electron Devices ED-27*:2217–2225.

Brunwin, R., Hamilton, B., Jordan, P., and Peaker, A. R. 1979. Detection of minority-carrier traps using transient spectroscopy. *Electron. Lett.* 15:349–350.

Day, D. S., Tsai, M. Y., Streetman, B. G., and Lang, D. V. 1979. Deep-level transient spectroscopy: System effects and data analysis. *J. Appl. Phys.* 50:5093–5098.

Dobaczewski, L., Peaker, A. R., and Bonde Nielsen, K. 2004. Laplace-transform deep-level spectroscopy: The technique and its applications to the study of point defects in semiconductors. *J. Appl. Phys.* 96:4689–4728.

Fairman, R. D., Morin, F. J., and Oliver, J. R. 1979. The influence of semi-insulating substrates on the electrical properties of high-purity GaAs buffer layers grown by vapor-phase epitaxy. *Inst. Phys. Conf. Ser.* 45:134–143.

Gafni, A., Modlin, R. L., and Brand, L. 1975. Analysis of fluorescence decay curves by means of the Laplace transformation. *Biophys. J.* 15:263–280.

Goto, G., Yanagisawa, S., Wada, O., and Takanashi, H. 1973. Determination of deep-level energy and density profiles in inhomogeneous semiconductors. *Appl. Phys. Lett.* 23: 150–151.

Halvorson, H. R. 1992. Padé–Laplace algorithm for sums of exponentials: Selecting appropriate exponential model and initial estimates for exponential fitting. *Methods Enzymol.* 210:54–67.

Hellen, E. H. 2005. Padé–Laplace analysis of signal averaged voltage decays obtained from a simple circuit. *Am. J. Phys.* 73:871–875.

Hurtes, Ch., Boulou, M., Mitonneau, A., and Bois, D. 1978. Deep-level spectroscopy in high-resistivity materials. *Appl. Phys. Lett.* 32:821–823.

Ikeda, K. and Takaoka, H. 1982. Deep level Fourier spectroscopy for determination of deep level parameters. *Jpn. J. Appl. Phys.* 21:462–466.

Johnson, N. M. 1982. Measurement of semiconductor-insulator interface states by constant-capacitance deep-level transient spectroscopy. *J. Vac. Sci. Technol.* 21:303–314.

Kimerling, L. C. 1976. New developments in defect studies in semiconductors. *IEEE Trans. Nucl. Sci.* NS-23:1497–1505.

Kirchner, P. D., Schaff, W. J., Maracas, G. N., Eastman, L. F., Chappel, T. I., and Ransom, C. M. 1981. The analysis of exponential and nonexponential transients in deep level transient spectroscopy. *J. Appl. Phys.* 52:6462–6470.

Kryzhniy, V. V. 2004. High-resolution exponential analysis via regularized numerical inversion of Laplace transforms. *J. Comput. Phys.* 199:618–630.

Lang, D. V. 1974. Deep-level transient spectroscopy: A new method to characterize traps in semiconductors. *J. Appl. Phys.* 45:3023–3032.

Lang, D. V. 1977. Review of radiation-induced defects in III–V compounds. *Inst. Phys. Conf. Ser.* 31:70–94.

Lang, D. V. 1979. Space-charge spectroscopy in semiconductors. *In Thermally Stimulated Relaxation in Solids* (P. Bräunlich, ed.), pp. 93–131. Springer-Verlag, Berlin, Heidelberg.

Look, D. C. 1983. The electrical and photoelectronic properties of semi-insulating GaAs. *In Semiconductors and Semimetals*, Vol. 19 (R. K. Willardson and A. C. Beer, eds.), pp. 75–170. Academic Press, New York.

Look, D. C. 1989. *Electrical Characterization of GaAs Materials and Devices*, p. 190. Wiley, New York.

Marco, S., Samitier, J., and Morante, J. R. 1995. A novel time-domain method to analyse multicomponent exponential transients. *Meas. Sci. Technol.* 6:135–142.

Miller, G. L., Lang, D. V., and Kimerling, L. C. 1977. Capacitance transient spectroscopy. *Annu. Rev. Mater. Sci.* 7:377–448.

Miller, G. L., Ramirez, J. V., and Ronbinson, D. A. H. 1975. A correlation method for semiconductor transient signal measurements. *J. Appl. Phys.* 46:2638–2644.

Milnes, A. G. 1973. *Deep Impurities in Semiconductors*. Wiley, New York.

Mitonneau, A., Martin, G. M., and Mircea, A. 1977. Investigation of minority deep levels by a new optical method. *Inst. Phys. Conf. Ser.* 33a:73–83.

Nolte, D. D. and Haller, E. E. 1987. Optimization of the energy resolution of deep level transient spectroscopy. *J. Appl. Phys.* 62:900–906.

Okushi, H. and Tokumaru, Y. 1980. Isothermal capacitance transient spectroscopy for determination of deep level parameters. *Jpn. J. Appl. Phys.* 19:L335–L338.

Petroff, P. M. and Lang, D. V. 1977. A new spectroscopic technique for imaging the spatial distribution of nonradiative defects in a scanning transmission electron microscope. *Appl. Phys. Lett.* 31:60–62.

Provencher, S. W. 1982. A constrained regularization method for inverting data represented by linear algebraic or integral equations. *Comput. Phys. Commun.* 27:213–227.

Rosencher, E. and Bois, D. 1982. Comparison of interface state density in MIS structure deduced from DLTS and Terman measurements. *Electron. Lett.* 18:545–546.

Sah, C. T., Forbes, L., Rosier, L. L., and Tasch, Jr., A. F. 1970. Thermal and optical emission and capture rates and cross sections of electrons and holes at imperfection centers in semiconductors from photo and dark junction current and capacitance experiments. *Solid State Electron.* 13: 759–788.

Smith, M. R., Cohn-Sfetcu, S., and Buckmaster, H. A., 1976. Decomposition of multicomponent exponential decays by spectral analytic techniques. *Technometrics* 18:467–482.

Takikawa, M. and Ikoma, T. 1980. Photo-excited DLTS: Measurement of minority carrier traps. *Jpn. J. Appl. Phys.* 19: L436–L438.

Tin, C. C., Barnes, P. A., Bardin, T. T., and Pronko, J. G. 1991a. Near-surface defects associated with 2.0-MeV $^{16}O^{+}$ ion implantation in n-GaAs. *J. Appl. Phys.* 70:739–743.

Tin, C. C., Barnes, P. A., Bardin, T. T., and Pronko, J. G. 1991b. Deep-level transient spectroscopy studies of 2.0 MeV $^{16}O^{+}$ ion implanted n-InP. *Nucl. Instrum. Methods* B59/60: 623–626.

Tin, C. C., Teh, C. K., and Weichman, F. L. 1987. Photoinduced transient spectroscopy and photoluminescence studies of copper contaminated liquid-encapsulated Czochralski-grown semi-insulating GaAs. *J. Appl. Phys.* 62:2329–2336.

Weiss, S. and Kassing, R. 1988. Deep level transient Fourier spectroscopy (DLTFS)—A technique for the analysis of deep level properties. *Solid State Electron.* 31:1733–1742.

Wessels, B. W. 1976. Determination of deep levels in Cu-doped GaP using transient-current spectroscopy. *J. Appl. Phys.* 47:1131–1133.

Yamasaki, K., Yoshida, M., and Sugano, T. 1979. Deep level transient spectroscopy of bulk traps and interface states in Si MOS diodes. *Jpn. J. Appl. Phys.* 18:113–122.

Yoshie, O. and Kamihara, M. 1983a. Photo-induced current transient spectroscopy in high-resistivity bulk material. I. Computer controlled multi-channel PICTS system with high-resolution. *Jpn. J. Appl. Phys.* 22:621–628.

Yoshie, O. and Kamihara, M. 1983b. Photo-induced current transient spectroscopy in high-resistivity bulk material. II. Influence of non-exponential transient on determination of deep trap parameters. *Jpn. J. Appl. Phys.* 22:629–635.

Yoshie, O. and Kamihara, M. 1985. Photo-induced current transient spectroscopy in high-resistivity bulk material. III. Scanning-PICTS system for imaging spatial distributions of deep-traps in semi-insulating GaAs wafer. *Jpn. J. Appl. Phys.* 24:431–440.

KEY REFERENCES

ASTM F978-90, 1993. See above.
Describes a standard procedure for DLTS.
Lang, 1974. See above.
A pioneering paper on DLTS.
Lang, 1979. See above.
A review of DLTS technique.
Miller et al., 1977. See above.
Provides an overview of various aspects of DLTS.
Ikeda and Takaoka, 1982. See above.
Weiss and Kassing, 1988. See above.
Articles detailing the Fourier transform technique.
Dobaczewski et al., 2004. See above.
Review current inverse Laplace technique and its applications.